Methods

Gene targeting, generation of mutant mice, and genotyping

Embryonic stem cells (CK35, provided by C. Kress[25]) were targeted with the constructs indicated in Fig. 1a as described previously[5]. Diphtheria toxin[5], or *PGK-DTA-bpA* (a gift from P. Soriano) and *PGK-puromycin-bpA* (a gift from A. Bradley) was used for selection in embryonic stem cells. The enhanced green fluorescent protein (EGFP) contains a Val164Ala mutation in pEGFP-C1 (Clontech; a gift from H. LeMouellic) and is followed by an SV40pA sequence. Both $Myf5^{nlacZ}$ and $Myf5^{GFP\text{-}P}$ comprise a *Sca*I–*Bst*YI deletion in exon 1 (122 amino acids) and thus lack the bHLH domain, whereas the floxed *Neo–Hygro* cassette in $Myf5^{NH}$ was an insertion at the *Sca*I site in exon 1 (residue 13). The remaining structure of *Myf5* is intact in all alleles. The two initiator ATG codons of *Myf5* in $Myf5^{NH}$ and $Myf5^{GFP\text{-}P}$ were mutated (ATG to GTG). The first ATG codons suitable for translation in $Myf5^{loxP}$ (residue 69, non-Kozak; residue 82, Kozak) are located in the chromatin remodelling (amino acids 39–78) and basic domains. $Myf5^{GFP\text{-}P/GFP\text{-}P}$, $Myf5^{loxP/loxP}$ and $Myf5^{nlacZ/loxP}$ were viable and were reduced in size. *Myod* (provided by M. Rudnicki[2]) and *Myf5* (129sv/C57BL6/DBA2) mutant mice were interbred to obtain double-mutant mice. A ubiquitously expressing PGKCre deleter strain (provided by Y. Lallemand[26]) was used to generate $Myf5^{loxP}$ and $Mrf4^{nlacZ\text{-}P/+}$:$Myf5^{loxP/+}$. *Mrf4* was targeted with an *nlacZ* reporter in embryonic stem cells previously targeted with, and *in cis* to, $Myf5^{NH}$ (data not shown). All embryos and mice were genotyped by Southern blotting or polymerase chain reaction (Supplementary Methods), and double mutants were genotyped again after sectioning. $Myf5^{nlacZ}$ and $Myf5^{GFP\text{-}P}$ allelic combinations were also phenotyped for mislocalized MPCs by staining with 5-bromo-4-chloro-3-indolyl β-D-galactopyranoside (X-Gal)[27] and GFP epifluorescence, respectively.

Processing of embryos and detection of transcripts and protein

Embryos were processed for WM-ISH or immunohistochemistry[13]. Riboprobes for *Myf5*, *Mrf4* and *Myod* were as described previously[13,28]. An *Mrf4* riboprobe spanning 421 base pairs (*Kpn*I–*Nde*I) was also used. For comparative WM-ISH experiments, age-matched and litter-matched embryos were used with independent probe sets and litters, and the ISH reactions were stopped at the same time. For protein detection by western blotting, the head and heart of E10.75 embryos were removed and lysates were prepared[29]. Primary polyclonal anti-Myf5 antibodies (dilution 1:500, carboxy-terminal specific; Santa Cruz) and secondary anti-rabbit peroxidase-conjugated secondary antibodies (dilution 1:40,000; Pierce) were applied and filters were treated with SuperSignal WestPico chemiluminescent substrate (Pierce).

Explant cultures and immunofluorescence

Micromass cultures were made as described previously[13], and time-lapse studies are described in Supplementary Methods. For immunofluorescence[27], two antibodies were used for Myf5 (polyclonal C-terminal[29], and a polyclonal, dilution 1:800; Santa Cruz), myogenin (F5D, monoclonal, dilution 1:5; Developmental Studies Hybridoma Bank, NICHD), Myod (monoclonal, dilution 1:100; Dako), myosin heavy chain (polyclonal, dilution 1:400; provided by G. Cossu) and desmin (monoclonal, dilution 1:100; Dako). Secondary antibodies were AlexaFluor 488 and 594 (Molecular Probes). For whole mount antibody staining see Supplementary Methods and http://www.pasteur.fr/recherche/unites/Csd. Images were taken either with a Zeiss Axiocam or Nikon numerical camera and a Zeiss fluorescent SZ11 or Axiophot microscope. Images were assembled in Adobe Photoshop and Indesign.

Received 13 March; accepted 23 July 2004; doi:10.1038/nature02876.

1. Tajbakhsh, S. Stem cells to tissue: molecular, cellular and anatomical heterogeneity in skeletal muscle. *Curr. Opin. Genet. Dev.* **13,** 412–422 (2003).
2. Rudnicki, M. A. *et al.* MyoD or myf-5 is required for the formation of skeletal muscle. *Cell* **75,** 1351–1359 (1993).
3. Kaul, A., Koster, M., Neuhaus, H. & Braun, T. Myf-5 revisited: loss of early myotome formation does not lead to a rib phenotype in homozygous Myf-5 mutant mice. *Cell* **102,** 17–19 (2000).
4. Kablar, B., Krastel, K., Tajbakhsh, S. & Rudnicki, M. A. Myf5 and MyoD activation define independent myogenic compartments during embryonic development. *Dev. Biol.* **258,** 307–318 (2003).
5. Tajbakhsh, S., Rocancourt, D. & Buckingham, M. Muscle progenitor cells failing to respond to positional cues adopt non-myogenic fates in *myf-5* null mice. *Nature* **384,** 266–270 (1996).
6. Kablar, B. *et al.* Myogenic determination occurs independently in somites and limb buds. *Dev. Biol.* **206,** 219–231 (1999).
7. Tajbakhsh, S. & Buckingham, M. The birth of muscle progenitor cells in the mouse: spatiotemporal considerations. *Curr. Top. Dev. Biol.* **48,** 225–268 (2000).
8. Weintraub, H. *et al.* The MyoD gene family: nodal point during specification of the muscle cell lineage. *Science* **251,** 761–766 (1991).
9. Braun, T., Rudnicki, M. A., Arnold, H. H. & Jaenisch, R. Targeted inactivation of the muscle regulatory gene Myf-5 results in abnormal rib development and perinatal death. *Cell* **71,** 369–382 (1992).
10. Tallquist, M. D., Weismann, K. E., Hellstrom, M. & Soriano, P. Early myotome specification regulates PDGFA expression and axial skeleton development. *Development* **127,** 5059–5070 (2000).
11. Kablar, B. *et al.* MyoD and Myf-5 differentially regulate the development of limb versus trunk skeletal muscle. *Development* **124,** 4729–4738 (1997).
12. Summerbell, D., Halai, C. & Rigby, P. W. Expression of the myogenic regulatory factor Mrf4 precedes or is contemporaneous with that of Myf5 in the somitic bud. *Mech. Dev.* **117,** 331–335 (2002).
13. Tajbakhsh, S., Rocancourt, D., Cossu, G. & Buckingham, M. Redefining the genetic hierarchies controlling skeletal myogenesis: *Pax-3* and *Myf-5* act upstream of *MyoD*. *Cell* **89,** 127–138 (1997).
14. Nabeshima, Y. *et al.* Myogenin gene disruption results in perinatal lethality because of severe muscle defect. *Nature* **364,** 532–535 (1993).
15. Rawls, A. *et al.* Overlapping functions of the myogenic bHLH genes MRF4 and MyoD revealed in double mutant mice. *Development* **125,** 2349–2358 (1998).
16. Moran, J. L. *et al.* Limbs move beyond the radical fringe. *Nature* **399,** 742–743 (1999).
17. Pham, C. T., MacIvor, D. M., Hug, B. A., Heusel, J. W. & Ley, T. J. Long-range disruption of gene expression by a selectable marker cassette. *Proc. Natl Acad. Sci. USA* **93,** 13090–13095 (1996).
18. Olson, E. N., Arnold, H.-H., Rigby, P. W. J. & Wold, B. J. Know your neighbors: three phenotypes in null mutants of the myogenic bHLH gene *MRF4*. *Cell* **85,** 1–4 (1996).
19. Hadchouel, J. *et al.* Modular long-range regulation of Myf5 reveals unexpected heterogeneity between skeletal muscles in the mouse embryo. *Development* **127,** 4455–4467 (2000).
20. Carvajal, J. J., Cox, D., Summerbell, D. & Rigby, P. W. A BAC transgenic analysis of the Mrf4/Myf5 locus reveals interdigitated elements that control activation and maintenance of gene expression during muscle development. *Development* **128,** 1857–1868 (2001).
21. Maroto, M. *et al.* Ectopic Pax-3 activates MyoD and Myf-5 expression in embryonic mesoderm and neural tissue. *Cell* **89,** 139–148 (1997).
22. Lu, J. R. *et al.* Control of facial muscle development by MyoR and capsulin. *Science* **298,** 2378–2381 (2002).
23. Wang, Y. & Jaenisch, R. Myogenin can substitute for Myf5 in promoting myogenesis but less efficiently. *Development* **124,** 2507–2513 (1997).
24. Bergstrom, D. A. & Tapscott, S. J. Molecular distinction between specification and differentiation in the myogenic basic helix–loop–helix transcription factor family. *Mol. Cell. Biol.* **21,** 2404–2412 (2001).
25. Kress, C., Vandormael-Pournin, S., Baldacci, P., Cohen-Tannoudji, M. & Babinet, C. Nonpermissiveness for mouse embryonic stem (ES) cell derivation circumvented by a single backcross to 129/Sv strain: establishment of ES cell lines bearing the Omd conditional lethal mutation. *Mamm. Genome* **9,** 998–1001 (1998).
26. Lallemand, Y., Luria, V., Haffner-Krausz, R. & Lonai, P. Maternally expressed PGK-Cre transgene as a tool for early and uniform activation of the Cre site-specific recombinase. *Transgenic Res.* **7,** 105–112 (1998).
27. Tajbakhsh, S. & Buckingham, M. E. Lineage restriction of the myogenic conversion factor myf-5 in the brain. *Development* **121,** 4077–4083 (1995).
28. Bober, E. *et al.* The muscle regulatory gene, Myf-6, has a biphasic pattern of expression during early mouse development. *J. Cell Biol.* **113,** 1255–1265 (1991).
29. Daubas, P., Tajbakhsh, S., Hadchouel, J., Primig, M. & Buckingham, M. Myf5 is a novel early axonal marker in the mouse brain and is subjected to post-transcriptional regulation in neurons. *Development* **127,** 319–331 (2000).

Supplementary Information accompanies the paper on **www.nature.com/nature**.

Acknowledgements We thank S. Shorte, E. Perret and P. Roux at the Pasteur Dynamic Imaging Center, and C. Cimper for assistance. The laboratories of S.T. and M.B. were funded by the Pasteur Institute, CNRS, AFM, ACI Integrative Biology programme of the French Ministry. M.B. was funded by the European Union. S.T. was also funded by grants from the HFSPO, Association pour la Recherche sur le Cancer. B.G.-M. received a fellowship from the ARC, and V.S. a grant from the Fondation pour la Recherche Médicale and Pasteur Institute. L.K.-D. was funded by the HFSPO, the EU and Pasteur Institute.

Competing interests statement The authors declare that they have no competing financial interests.

Correspondence and requests for materials should be addressed to S.T. (shaht@pasteur.fr).

Exogenous control of mammalian gene expression through modulation of RNA self-cleavage

Laising Yen[1], Jennifer Svendsen[1], Jeng-Shin Lee[1], John T. Gray[1], Maxime Magnier[1], Takashi Baba[2], Robert J. D'Amato[2] & Richard C. Mulligan[1]

[1]*Department of Genetics, Harvard Institute of Human Genetics, Harvard Medical School, and Division of Molecular Medicine and*
[2]*Department of Surgery, Children's Hospital, Boston, Massachusetts 02115, USA*

Recent studies on the control of specific metabolic pathways in bacteria have documented the existence of entirely RNA-based mechanisms for controlling gene expression. These mechanisms involve the modulation of translation, transcription termination or RNA self-cleavage through the direct interaction of specific intracellular metabolites and RNA sequences[1–4]. Here we show that an analogous RNA-based gene regulation system can effectively be designed for mammalian cells via the incorporation of sequences encoding self-cleaving RNA motifs[5] into the transcriptional unit of a gene or vector. When correctly positioned, the sequences lead to potent inhibition of gene or vector expression,

owing to the spontaneous cleavage of the RNA transcript. Administration of either oligonucleotides complementary to regions of the self-cleaving motif or a specific small molecule results in the efficient induction of gene expression, owing to inhibition of self-cleavage of the messenger RNA. Efficient regulation of transgene expression is shown in a variety of mammalian cell lines and live animals. In conjunction with other emerging technologies[6], this methodology may be particularly applicable to the development of gene regulation systems tailored to any small inducer molecule, and provide a novel means of biological sensing *in vivo* that may have an important application in the regulated delivery of protein therapeutics.

The general strategy for controlling gene expression through modulation of RNA processing is shown in Fig. 1a. The approach is critically dependent on both the ability of a specific self-cleaving ribozyme to efficiently cleave (>99%) an mRNA molecule in which it is embedded, and the availability of a small molecule capable of efficiently inhibiting self-cleavage of the cis-acting ribozyme within an intracellular milieu. Candidate ribozyme sequences capable of efficient cleavage in mammalian cells were identified using a transient transfection assay which makes use of a standard mammalian expression vector[7] which encodes a LacZ reporter (Fig. 1b). Candidate ribozyme sequences were introduced into one of a number of different locations within the vector transcriptional unit, and, in parallel, the corresponding inactive mutant ribozymes were introduced into the same sites to measure the efficiency of reduction of reporter gene expression. After transfection of human embryonic kidney (HEK) 293 cells with these vectors, protein extracts were prepared from cells and the β-gal level quantified. Cleavage activity of the functional ribozyme in cells was measured as 'fold' suppression in reporter gene expression relative to the vector with inactive ribozyme.

A large number of different ribozyme encoding motifs were chosen for analysis, including un-manipulated natural ribozyme sequences, ribozymes shown to function in mammalian cells and ribozymes engineered by others to possess specific biochemical or catalytic properties *in vitro* (for example, high K_{cat}, low Mg^{2+} requirement, and so on; see Supplementary Table 1). Although the vast majority of ribozymes tested did not appreciably affect reporter expression, as reflected by near equal expression of LacZ by vectors encoding functional and inactive ribozymes (defined as fold = 1), two ribozyme motifs were identified which did seem to function effectively: the hammerhead Pst-3 ribozyme derived from the *Dolichopoda* cave cricket[8] (Fig. 1c; 13-fold difference between functional and inactive ribozyme) and the hammerhead Sm1 ribozyme derived from the trematode *Schistosoma mansoni*[9] (Fig. 1d) in which the tetraloop 5′UUCG 3′ was grafted onto an extended stem III (19-fold difference). Interestingly, both ribozymes possess unique structures relative to the other hammerhead ribozymes tested, in that they contain an extended stem-I with an internal loop (see Fig. 1c, d).

Based on its apparent higher level of self-cleavage activity, the Sm1 ribozyme was chosen for further study and manipulation. In an effort to improve the efficiency of the Sm1 ribozyme self-cleavage activity, a series of modifications of the Sm1 ribozyme structure were made and evaluated. As shown in Fig. 1d, specific modification at nucleotide 7 (C to U) in the conserved catalytic core[10], and changes in distal stem III led to a significant increase in the extent of self-cleavage (the modified Sm1 ribozyme was termed N73, up to 62-fold difference between functional and inactive ribozyme). Transfer of the N73 ribozyme from position A to E of the vector enhanced the activity to 225-fold (this ribozyme was termed N79 and was used in the subsequent studies). Additional modifications of stem I near the catalytic core and near the restriction insertion site led to further increases in activity, resulting ultimately in an overall 1,401-fold difference in expression levels between functional verses inactive ribozyme (Fig. 1e).

In addition to modifications that led to improved self-cleavage activity, several modifications, notably those involving the shortening of stem I (Fig. 1f) and alteration of nucleotides within the internal loop of stem I (Fig. 1g), dramatically reduced the level of self-cleavage. Interestingly, neither of those two modifications affect conserved core sequences known to be required for ribozyme cleavage *in vitro*[11]. Under standard *in vitro* conditions of 10 mM Mg^{2+}, measurement of the catalytic activity of N79 ribozyme and N107(U to G) ribozyme (which carries a single base U to G change in the loop I and is inactive in mammalian cells, Fig. 1g) indicated that both enzymes were equally functional *in vitro* (K_{obs} values of $0.84\,min^{-1}$ and $1.06\,min^{-1}$, respectively; see Supplementary Methods). Intriguingly, determination of the cleavage rate under low Mg^{2+} conditions (0.5 mM Mg^{2+}) indicated that only the N79 enzyme possessed significant activity (N79 $K_{obs} = 0.84\,min^{-1}$ verses N107(U to G) $K_{obs} = 0.014\,min^{-1}$). These results suggest that sequences within the unique loop structure of stem-I of the Sm1 ribozyme may enable efficient self-cleavage in mammalian cells in part because they facilitate self-cleavage at physiological Mg^{2+} concentrations. Consistent with this idea, measurement of the K_{obs} of another well-characterized hammerhead ribozyme[12] ('McSwiggen's hammerhead'; see Supplementary Table 1) previously shown by others to function in mammalian cells, but shown in our transfection assay to possess no appreciable activity, indicated that significant *in vitro* cleavage activity occurred only under high Mg^{2+} conditions ($0.32\,min^{-1}$ at 10 mM Mg^{2+} verses $0.015\,min^{-1}$ at 0.5 mM Mg^{2+}). However, to what extent the ability to function at low Mg^{2+} concentration *per se* contributes to the ability of a ribozyme to function efficiently in mammalian cells remains unclear, because several ribozymes engineered by others to efficiently function *in vitro* under low Mg^{2+} conditions[13,14] were among the many ribozymes that were found to be non-functional in our transient transfection assay (Supplementary Table 1).

In addition to functioning in HEK293 cells within the context of the original cytomegalovirus (CMV)-based pMD vector tested, the N79 ribozyme also dramatically reduced β-gal expression in a variety of other commonly used cell lines after transfection (Fig. 2a). In addition, the N79 ribozyme was able to function efficiently when placed within other transcriptional units which made use of different promoters and a different reporter gene (enhanced green fluorescent protein, eGFP) (Fig. 2b). As we had observed in the primary screen of different ribozyme motifs for activity in mammalian cells, N79 was able to function when placed in several, but not all locations of the pMD transcriptional unit, albeit at different efficiencies (Fig. 2c). Importantly, placement of two ribozyme sequences in tandem, in some cases (for example, position E) led to a dramatic suppression of reporter gene expression (Fig. 2c).

An essential requirement for the development of a gene regulation system based on modulation of self-cleavage activity is the availability of small inducer molecules capable of efficient inhibition of ribozyme activity in mammalian cells. In an effort to identify such molecules, we first surveyed a large number of common antibiotics that had been shown to inhibit ribozyme cleavage *in vitro*[15–20]. In no case was significant inhibition of self-cleavage by these antibiotics observed in our transient transfection assay (data not shown). We next surveyed the ability of different types of antisense oligonucleotides[21] to inhibit ribozyme cleavage (see Fig. 1e for targeted sequence). Whereas transfection with peptide nucleic acids, locked nucleic acids and 'grip' nucleic acids had no measurable effects on self-cleavage activity, transfection with phosphorothiolate, 2′-O-methyl and phosphorothiolate 2′-O-methyl derived RNAs led to modest inhibition of self-cleavage (<tenfold induction). In contrast, transfection of a morpholino oligonucleotide[22] led to a strong inhibition of ribozyme self-cleavage, as demonstrated by a dramatic increase in reporter gene expression (Fig. 3a). The 'fold' induction afforded by this method was somewhat variable

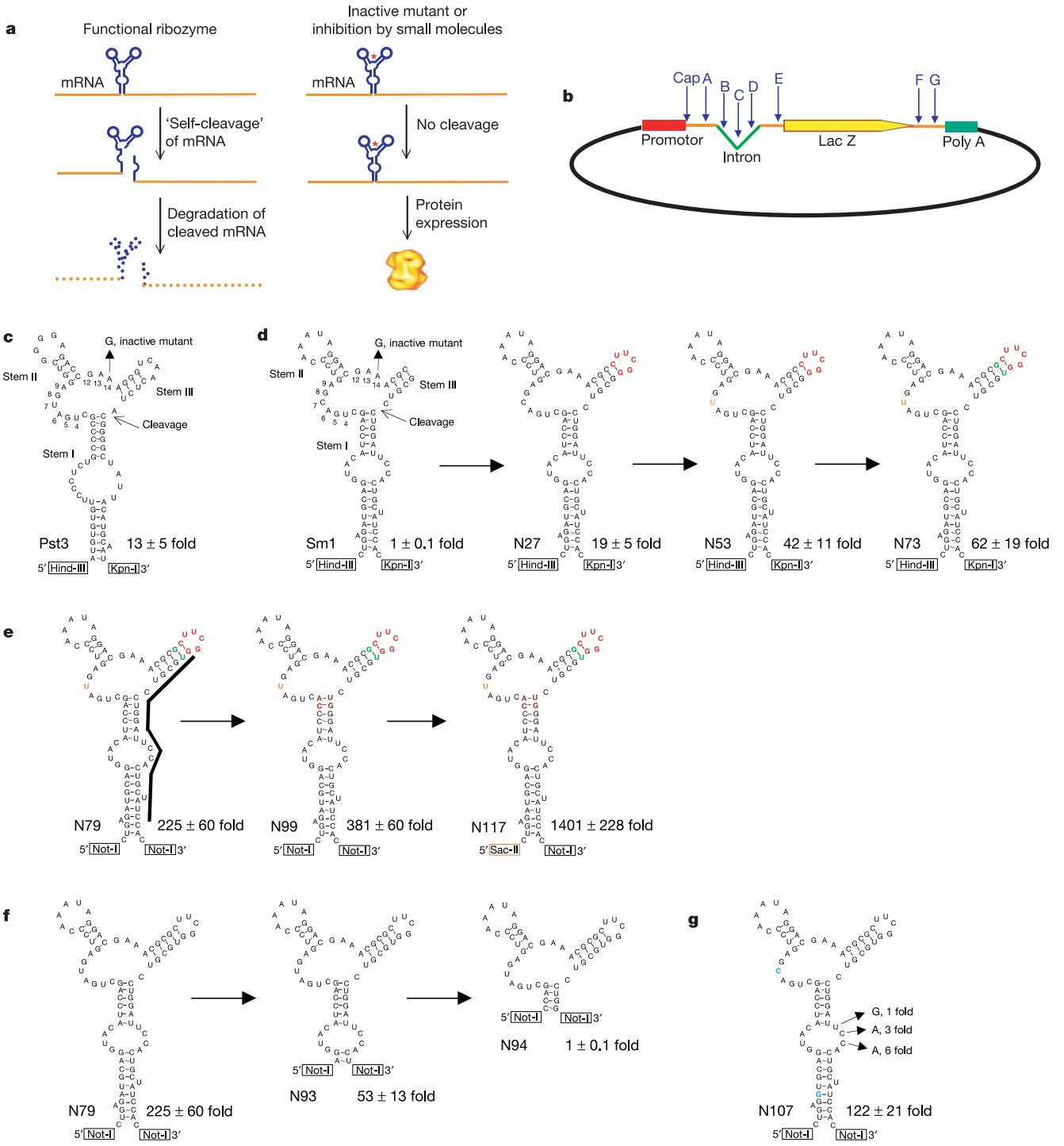

Figure 1 Strategy for controlling gene expression through the modulation of RNA self-cleavage and optimization of Schistosome Sm1 ribozyme self-cleavage activity. **a**, When a cis-acting hammerhead ribozyme is embedded in the mRNA, self-cleavage leads to the destruction of the mRNA and the absence of gene expression. However, an inactive mutant or the administration of specific inhibitors of the ribozyme leads to the generation of intact mRNA's and protein expression. **b**, The reporter gene expression vector pMD used for transfection assay, and the positions where ribozyme were placed. Cap site at the very beginning of the mRNA; A site upstream of the intron; B,C, and D site in the intron; E site immediately upstream of the translation start; F and G sites in the 3′-untranslated region. **c**–**g**, Optimization of Schistosome Sm1 activity. Ribozyme inserted at position A of pMD vector (**c**, **d**) and at position E of vector (**e**–**g**). Corresponding inactive mutants contained an A14 to G substitution. Name of ribozyme is shown at left; cleavage activity at right. Cricket Pst3 motif (**c**). Nucleotide numbering follows nomenclature of Hertel *et al.*[10]. *Schistosome* Sm1 motif (**d**). The original Sm1 lacked loop III and exhibited no activity in cells. Nucleotides depicted in colour reflect changes made to Sm1. Changes in stem I of N79 near the core or near the restriction insertion site further enhanced activity (**e**). Black line identifies the sequence targeted by antisense morpholino oligonucleotides. Shortening of stem I vastly reduced ribozyme cleavage activity (**f**). Single nucleotide changes in loop I of the N107 ribozyme decreased its activity dramatically (**g**). The N107 ribozyme is a variant of N79 in which two 'AUG' were replaced by GUG and ACG to eliminate the potential start codons. The mean ± s.d. of at least four independent measurements is shown.

from experiment to experiment (110–2000-fold in the case of the double N79 construct), probably because of the variability of efficiency of delivery and toxicity associated with transfection of the oligonucleotide. However, the extent of induction of gene expression was nonetheless comparable to that achieved with other gene regulation systems, and clearly represents a range that would be useful for a variety of experimental and clinical settings. In some cases, the absolute levels of gene expression achieved after morpholino administration approached 50% of the theoretical maximum induction possible (that is, the level of gene expression produced by the inactive ribozyme), suggesting that ribozyme cleavage can be very efficiently inhibited in mammalian cells.

To identify small molecules capable of inhibiting ribozyme self-cleavage, we generated stable cell lines carrying an integrated expression construct in which a luciferase reporter was placed under the control of two copies of the N79 ribozyme, and made use of the cells in high-throughput screening studies (L.Y., M.M., Y. Tang, R. Weissleder, B. R. Stockwell and R.C.M., unpublished observations). Of the several compounds identified, toyocamycin[23] (a nucleoside analogue) was found to be the most potent inhibitor of ribozyme function. As shown in Fig. 3b, administration of 1.5 μM toyocamycin to the cells led to a dramatic increase in luciferase protein expression. A parallel analysis of luciferase mRNA expression demonstrated that in the absence of drug, little if any luciferase mRNA was produced in the nucleus or cytoplasm, whereas in drug-treated cells, the amount of luciferase mRNA was increased to a level comparable to that of cells carrying inactive ribozyme (Fig. 3c). The lack of detectable mRNA in untreated cells suggests that cleaved mRNAs are rapidly degraded, presumably because the cleaved fragments lack conventional sequences at the ends of mRNAs. In contrast to toyocamycin, a related compound, adenosine, possessed no ability to inhibit ribozyme self-cleavage (data not shown). Although the above assays indicate that self-cleavage is highly efficient in the stable cell line, sensitive measurement of luciferase activity by photon emission indicates that there is, nevertheless, an extremely low but detectable amount of luciferase expression above the background emission level of control cells that carry no luciferase gene (see legend to Fig. 3).

Having documented the ability of the ribozyme-based regulation

a

	Kidney	Cervical cancer	Melanoma	Ovary	Fibroblast
Type of cells	293T	Hela	B16	CHO	3T3
Functional Rz	0.27	0.00	0.03	0.00	0.00
Inactive Rz	109.6	8.8	22.8	10.0	7.6
Fold Decrease	403	N/A*	671	N/A*	N/A*

* The reporter gene activity of functional ribozyme construct was undetectable.

b

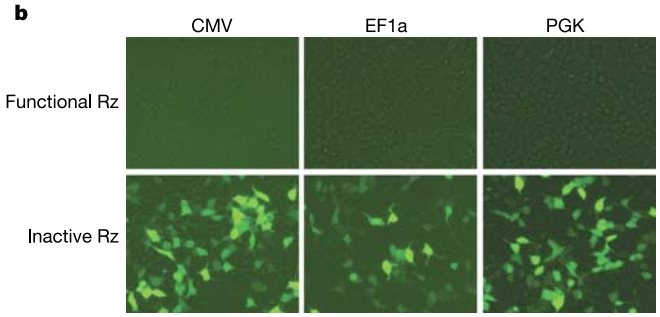

c

Position	5′ UTR Cap	A	E	Intron B	C	D	3′ UTR F	G
Single N79	102 ± 17	62 ± 19	225 ± 60	2 ± 1	3 ± 1	3 ± 1	4 ± 2	3 ± 1
Double N79	205 ± 56	44 ± 7	3183 ± 717				6 ± 1	

Figure 2 Efficient self-cleavage can occur in different cells, with different vectors and with ribozyme sequences positioned in different locations. **a**, N79 functioned efficiently in a variety of cell types. Numbers are the measurements of β-gal expressed. **b**, N79 functioned efficiently with CMV, EF1a and PGK promoters in a vector encoding the eGFP reporter. **c**, N79 functioned efficiently at some but not all positions within the vector. Numbers are 'fold decrease' in β-gal expression (functional verses inactive ribozyme). The mean ± s.d. from at least four independent measurements is shown.

a

Induction	In fold	By percentage
Single N79	31	27%
	23	35%
	69	34%
Double N79	2012	38%
	851	50%
	110	5%
	200	5%

b

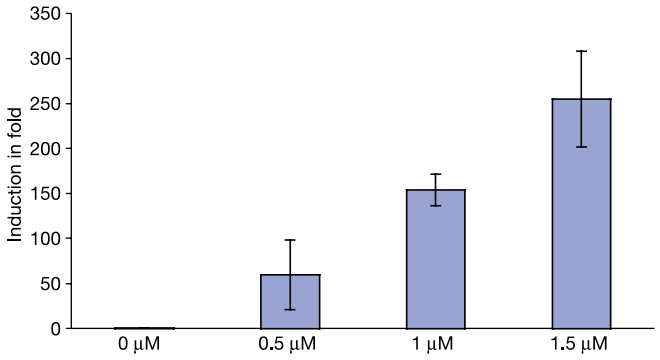

c

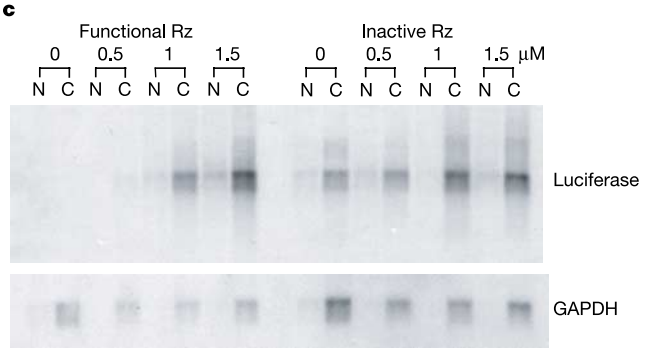

Figure 3 Induction of gene expression in cultured cells through inhibition of ribozyme self-cleavage. **a**, Effect of morpholino oligonucleotide on N79 ribozyme in transient transfection assay. Induction was measured by 'fold increase' in β-gal expression with or without morpholino application. The level of induction is also shown as a percentage relative to the expression level of inactive ribozyme. The target for the oligonucleotide is shown in Fig. 1e. **b**, Induction of luciferase expression by toyocamycin in a stable cell line carrying an expression construct containing a double N79 ribozyme. Cells were treated with toyocamycin for 24 h at dosage of 0, 0.5, 1 and 1.5 μM (toxic effects were observed at concentrations higher than 1.5 μM). Quantitative measurements of luciferase activity revealed emission of 1555, 66774, 242546 and 377655 photons per second per 1,000 cells respectively, as compared to a background emission of 121 from cells carrying no luciferase gene. Values are mean ± s.d. from at least four independent measurements. **c**, Induction by toyocamycin at the RNA level as shown by northern blot analyses. Experimental conditions were similar to that of **b**. RNA was purified from the nucleus (N) or the cytoplasm (C) after 24 h of treatment.

system to function in mammalian cell culture, an important issue was whether the intracellular machinery and 'environment' necessary for self-cleavage was operable in primary cells *in vivo*. To address this issue, we generated recombinant adeno-associated virus (AAV) genomes carrying transcription units derived from pMD ribozyme–luciferase vectors (possessing two copies of functional or inactive N79 ribozyme at the E position), and prepared high titre virus possessing the host range of AAV serotype 5. The two viruses were then used to inject nude mice sub-retinally as described in Supplementary Methods. To provide a means of normalization for differences in the capacity to measure luciferase activity on different days (such as, variations due to the delivery of the luciferin substrate), all animals were also injected in the hamstring muscles of the hind limb with AAV viruses carrying the inactive N79 ribozymes. After 21 days, the injected animals were imaged for luciferase gene expression using the Xenogen IVIS imager (which provides a quantitative measure of luciferase expression based on single-photon detection)[24]. Immediately after imaging, cohorts of mice injected with virus carrying the functional ribozyme sequences were implanted under the dorsal skin with seven day 'time-release' pellets of either toyocamycin or adenosine, whereas another cohort of mice injected with virus carrying the inactive ribozyme sequences were implanted with toyocamycin pellets. Two days later, all animals were then imaged for luciferase expression.

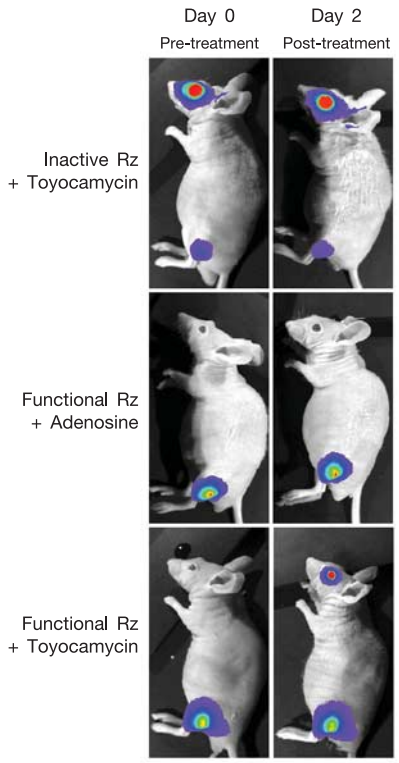

Figure 4 Effective control of gene expression *in vivo* using ribozyme-based gene regulation system. Upper panels show animal in which retina was injected with AAV carrying double inactive N79 and treated with toyocamycin. Middle panels show animal in which retina was injected with AAV carrying double functional N79 and treated with adenosine. Lower panels show same as middle panel but treated with toyocamycin. A strong induction in luciferase expression at day 2 was observed in lower panel. Animals were also injected in the hamstring muscles of the hind limb with AAV carrying double inactive N79 as internal control. AAV injection was done 3 weeks before the first imaging day (day 0). Drug-releasing pellets were implanted subcutaneously in the dorsal neck immediately after the first imaging, and released the drug over 7 days. The toyocamycin pellet contains 10 μg of drug; adenosine pellet 50 μg.

Representative images of mice in each treatment group, taken before and after drug treatment, are shown in Fig. 4. The images demonstrate that, as expected, mice injected with virus carrying inactive ribozymes showed robust luciferase expression in the retina, and the expression was independent of the administration of toyocamycin (Fig. 4, upper panel). Mice injected with virus carrying two functional ribozymes and implanted with adenosine pellets showed little if any gene expression before or after adenosine treatment (Fig. 4, middle panel), consistent with the inability of adenosine to inhibit ribozyme self-cleavage. Importantly, mice injected with virus carrying the functional ribozymes showed readily detectable expression only after toyocamycin treatment (Fig. 4, lower panel). Quantification of the photon output indicated gene expression was 'induced' 39, 185 and 191-fold in the three mice infected with virus carrying the functional ribozymes and treated with toyocamycin. In the last case (animal showing 191-fold induction) the induced gene expression reached a level within 40% of the gene expression of virus carrying inactive ribozymes. These results indicate that significant ribozyme-mediated gene regulation can be accomplished in the *in vivo* setting. Whereas the retina may be particularly accessible to 'inducer' due to its extensive vascularization, we have shown in preliminary experiments that gene regulation can be accomplished at a number of other anatomical sites *in vivo* (unpublished observations).

Overall, the studies reported here provide an important 'proof-of-principle' for gene regulation strategies based on the modulation of RNA processing. Specifically, the fact that efficient ribozyme self-cleavage can occur in a variety of mammalian cell lines and in primary cells *in vivo*, suggests that mammalian cells may in general be 'permissive' for efficient ribozyme self-cleavage. Therefore, ribozyme-based regulation systems may be generally applicable to the manipulation of gene expression in cells and animals. In addition to the implications for the development of gene regulation strategies, the studies also provide a compelling rationale for determining whether 'naturally occurring' RNA-only mechanisms for gene regulation exist in mammalian cells.

The most commonly used systems for controlling gene expression, that rely on the regulation of transcription[25–28], have proved to be extremely powerful experimental tools. However, despite their utility, such systems possess at least some practical and theoretical limitations because of their reliance on chimaeric transcriptional transactivators and specialized promoter elements. These limitations include: (1) the need to co-introduce expression constructs for both the transactivator and the transgene to be regulated; (2) the potential toxicities due to expression of a chimaeric transactivator; (3) difficulties in application of such systems to the regulation of endogenous cellular genes due to the requirement of a specialized promoter; and (4) the limited number of small inducer molecules available for experimental and therapeutic applications.

In contrast to systems based on the regulation of transcription, the ribozyme-based system we have described does not require the expression of any protein transactivator products and is not dependent on the use of any specialized promoter elements. Therefore, in theory, this system represents a 'portable' regulation system that could be 'embedded' into any endogenous gene or engineered vector transcription unit. Although the two inhibitors of ribozyme self-cleavage we have described may not be ideal for many experimental applications, it is likely that additional inducers with more desirable pharmacokinetic properties and toxicity profiles can be identified through high-throughput screening efforts and further evaluation of specific antisense oligonucleotides and *in vivo* delivery methods to cells. In addition, recent studies have shown that it is possible to generate ribozymes whose *in vitro* self-cleavage activity is controlled by a specific ligand, either by the 'judicious' linkage of RNA aptamer sequences to specific regions of hammerhead ribozyme[29], or through the use of *in vitro* evolution technologies[30].

Application of these technologies to the strategy for controlling gene expression described here should make it possible in the future to tailor specific ribozyme-based gene regulation systems to any small molecule ligand. Such an approach would provide a general methodology for developing gene regulation systems which rely on ligands with desirable and/or specific pharmacokinetic properties. In addition, the combined technologies should provide the means to independently and simultaneously control the expression of multiple gene products, and to express gene products in response to the concentration of any intracellular molecule or combinations of molecules. Such a form of biological sensing could have broad experimental and therapeutic applications. □

Methods

Transient reporter expression assay

Plasmids carrying different ribozymes were transfected into HEK293T cells, which were lysed after 24 h. The cell extracts were incubated with ONPG (o-nitrophenyl-β-D-galactopyranoside), and the amount of β-galactosidase was measured by quantifying the processed ONPG using a luminometer.

Catalytic rate measurement

Ribozymes were generated by *in vitro* transcription in the presence of 50 μM blocking antisense oligonucleotides. Full length ribozymes were purified and the cleavage rate determined in 50 mM Tris-HCl, pH 7.5 at 23 °C. K_{obs} was calculated according to the equation $F_t = F_0 + F_\infty(1 - e^{kt})$, where F_0 and F_∞ are the cleavage fractions at zero time and at the reaction endpoint, and k is the first order rate constant of cleavage (K_{obs}).

Non-invasive bioluminescent imaging

Before imaging, the anaesthetized mice were injected with 150 μl of luciferin (30 mg ml^{-1}) and the pupils were moistened and dilated with 1% tropicamide. A series of bioluminescent images were taken for up to 30 min using the Xenogen IVIS imager. Photon output was quantified at the plateau of the time course using the LivingImage software. Induction in fold was calculated based on the photon output in the retina before and after drug treatment, and was normalized to the photon output from the leg muscles. See Supplementary Information for more detailed Methods.

Received 25 May; accepted 14 July 2004; doi:10.1038/nature02844.

1. Winkler, W., Nahvi, A. & Breaker, R. R. Thiamine derivatives bind messenger RNAs directly to regulate bacterial gene expression. *Nature* **419,** 952–956 (2002).
2. Winkler, W. C., Nahvi, A., Roth, A., Collins, J. A. & Breaker, R. R. Control of gene expression by a natural metabolite-responsive ribozyme. *Nature* **428,** 281–286 (2004).
3. Mandal, M. & Breaker, R. R. Adenine riboswitches and gene activation by disruption of a transcription terminator. *Nature Struct. Mol. Biol.* **11,** 29–35 (2004).
4. Cech, T. R. RNA finds a simpler way. *Nature* **428,** 263–264 (2004).
5. Cech, T. R. Nobel lecture. Self-splicing and enzymatic activity of an intervening sequence RNA from *Tetrahymena*. *Biosci. Rep.* **10,** 239–261 (1990).
6. Silverman, S. K. Rube Goldberg goes (ribo)nuclear? Molecular switches and sensors made from RNA. *RNA* **9,** 377–383 (2003).
7. Ory, D. S., Neugeboren, B. A. & Mulligan, R. C. A stable human-derived packaging cell line for production of high titer retrovirus/vesicular stomatitis virus G pseudotypes. *Proc. Natl Acad. Sci. USA* **93,** 11400–11406 (1996).
8. Rojas, A. A. *et al.* Hammerhead-mediated processing of satellite pDo500 family transcripts from *Dolichopoda* cave crickets. *Nucleic Acids Res.* **28,** 4037–4043 (2000).
9. Ferbeyre, G., Smith, J. M. & Cedergren, R. *Schistosome* satellite DNA encodes active hammerhead ribozymes. *Mol. Cell. Biol.* **18,** 3880–3888 (1998).
10. Hertel, K. J. *et al.* Numbering system for the hammerhead. *Nucleic Acids Res.* **20,** 3252 (1992).
11. Ruffner, D. E., Stormo, G. D. & Uhlenbeck, O. C. Sequence requirements of the hammerhead RNA self-cleavage reaction. *Biochemistry* **29,** 10695–10702 (1990).
12. Chowrira, B. M., Pavco, P. A. & McSwiggen, J. A. *In vitro* and *in vivo* comparison of hammerhead, hairpin and hepatitis delta virus self-processing ribozyme cassettes. *J. Biol. Chem.* **269,** 25856–25864 (1994).
13. Zillmann, M., Limauro, S. E. & Goodchild, J. *In vitro* optimization of truncated stem-loop II variants of the hammerhead ribozyme for cleavage in low concentrations of magnesium under non-turnover conditions. *RNA* **3,** 734–747 (1997).
14. Conaty, J., Hendry, P. & Lockett, T. Selected classes of minimised hammerhead ribozyme have very high cleavage rates at low Mg^{2+} concentration. *Nucleic Acids Res.* **27,** 2400–2407 (1999).
15. Hermann, T. & Westhof, E. Aminoglycoside binding to the hammerhead ribozyme: a general model for the interaction of cationic antibiotics with RNA. *J. Mol. Biol.* **276,** 903–912 (1998).
16. Jenne, A. *et al.* Rapid identification and characterization of hammerhead-ribozyme inhibitors using fluorescence-based technology. *Nature Biotechnol.* **19,** 56–61 (2001).
17. Murray, J. B. & Arnold, J. R. Antibiotic interactions with the hammerhead ribozyme:tetracyclines as a new class of hammerhead inhibitor. *Biochem. J.* **317,** 855–860 (1996).
18. Stage, T. K., Hertel, K. J. & Uhlenbeck, O. C. Inhibition of the hammerhead ribozyme by neomycin. *RNA* **1,** 95–101 (1995).
19. Tor, Y., Hermann, T. & Westhof, E. Deciphering RNA recognition: aminoglycoside binding to the hammerhead ribozyme. *Chem. Biol.* **5,** R277–R283 (1998).
20. von Ahsen, U., Davies, J. & Schroeder, R. Antibiotic inhibition of group I ribozyme function. *Nature* **353,** 368–370 (1991).
21. Braasch, D. A. & Corey, D. R. Novel antisense and peptide nucleic acid strategies for controlling gene expression. *Biochemistry* **41,** 4503–4510 (2002).
22. Morcos, P. A. Achieving efficient delivery of morpholino oligos in cultured cells. *Genesis* **30,** 94–102 (2001).
23. Aszalos, A., Lemanski, P., Robison, R., Davis, S. & Berk, B. Identification of antibiotic 1037 as toyocamycin. *J. Antibiot. (Tokyo)* **19,** 285 (1966).
24. Contag, P. R., Olomu, I. N., Stevenson, D. K. & Contag, C. H. Bioluminescent indicators in living mammals. *Nature Med.* **4,** 245–247 (1998).
25. Gossen, M. & Bujard, H. Tight control of gene expression in mammalian cells by tetracycline-responsive promoters. *Proc. Natl Acad. Sci. USA* **89,** 5547–5551 (1992).
26. Rivera, V. M. *et al.* A humanized system for pharmacologic control of gene expression. *Nature Med.* **2,** 1028–1032 (1996).
27. Suhr, S. T., Gil, E. B., Senut, M. C. & Gage, F. H. High level transactivation by a modified *Bombyx* ecdysone receptor in mammalian cells without exogenous retinoid X receptor. *Proc. Natl Acad. Sci. USA* **95,** 7999–8004 (1998).
28. Wang, Y., O'Malley, B. W. Jr, Tsai, S. Y. & O'Malley, B. W. A regulatory system for use in gene transfer. *Proc. Natl Acad. Sci. USA* **91,** 8180–8184 (1994).
29. Breaker, R. R. Engineered allosteric ribozymes as biosensor components. *Curr. Opin. Biotechnol.* **13,** 31–39 (2002).
30. Wilson, D. S. & Szostak, J. W. *In vitro* selection of functional nucleic acids. *Annu. Rev. Biochem.* **68,** 611–647 (1999).

Supplementary Information accompanies the paper on **www.nature.com/nature**.

Acknowledgements We thank K. Salehi-Ashtlani and J. Szostak for helpful discussions, Y. Tang and R. Weissleder for help with imaging experiments performed during the early course of the work, and M. Chung for her technical assistance. This work was supported by grants from AMGEN and L'Association Francaise contre les Myopathies (AFM). R.C.M. is an AMGEN consultant and equity holder.

Competing interests statement The authors declare competing financial interests: details accompany the paper on **www.nature.com/nature**.

Correspondence and requests for materials should be addressed to R.M. (mulligan@receptor.med.harvard.edu).

Tropism switching in *Bordetella* bacteriophage defines a family of diversity-generating retroelements

Sergei Doulatov[1]*, Asher Hodes[1]*, Lixin Dai[3], Neeraj Mandhana[1], Minghsun Liu[1], Rajendar Deora[1], Robert W. Simons[1,2], Steven Zimmerly[3] & Jeff F. Miller[1,2]

[1]*Department of Microbiology, Immunology and Molecular Genetics, David Geffen School of Medicine at UCLA, and*
[2]*The Molecular Biology Institute, University of California, Los Angeles, California 90095, USA*
[3]*Department of Biological Sciences, University of Calgary, Calgary, Alberta T2N 1N4, Canada*

* These authors contributed equally to this work

Bordetella **bacteriophages generate diversity in a gene that specifies host tropism[1]. This microevolutionary adaptation is produced by a genetic element that combines the basic retroelement life cycle of transcription, reverse transcription and integration with site-directed, adenine-specific mutagenesis. Central to this process is a reverse transcriptase-mediated exchange between two repeats; one serving as a donor template (TR) and the other as a recipient of variable sequence information (VR)[1]. Here we describe the genetic basis for diversity generation. The directionality of information transfer is determined by a 21-base-pair sequence present at the 3′ end of VR. On the basis of patterns of marker transfer in response to variant selective pressures, we propose that a TR reverse transcript is mutagenized, integrated into VR as a single non-coding strand, and then partially converted to the parental VR sequence. This allows the diversity-generating system to minimize variability to the subset of bases under selection. Using the *Bordetella* phage**